Strong Field Quantum Path Control Using Attosecond Pulse Trains

Kenneth J. Schafer and Mette B. Gaarde
Department of Physics and Astronomy, Louisiana State University, Baton Rouge, Louisiana 70803-4001, USA

Arne Heinrich, Jens Biegert, and Ursula Keller
Physics Department, Swiss Federal Institute of Technology (ETH), CH-8093 Zürich, Switzerland
(Received 2 September 2003; published 16 January 2004)

We show that attosecond pulse trains have a natural application in the control of strong field processes. In combination with an intense infrared laser field, the pulse train can be used to microscopically select a single quantum path contribution to a process that would otherwise consist of several interfering components. We present calculations that demonstrate this by manipulating the time-frequency properties of high order harmonics at the single atom level. This quantum path selection can also be used to define a high resolution attosecond clock.

DOI: 10.1103/PhysRevLett.92.023003 PACS numbers: 32.80.Wr, 32.80.Qk, 42.65.Ky

It has recently been experimentally demonstrated that a train of pulses as short as a few hundred attoseconds is produced when several odd harmonics of an intense infrared (IR) laser field are phase locked [1]. The periodicity of the resulting attosecond pulse train (APT) is half the fundamental IR cycle [2,3]. In this Letter we show that this periodicity makes the APT a natural tool for controlling strong field processes driven by the IR laser. The efficacy of this control mechanism can best be appreciated in the framework of the successful semiclassical description of intense laser-matter interactions [4]. In this picture, the amplitude for any strong field process can be expressed as a coherent sum over only a few quantum orbits [5]. These space-time trajectories follow a sequence of release into the continuum (ionization), acceleration in the IR field, and return to the ion core, where the electron can either rescatter or recombine. When an APT is used in combination with an IR laser, the short duration of the attosecond pulses fixes the ionization to a particular point in each IR half cycle and allows us to select which quantum paths are available for the electron to follow.

In this Letter we demonstrate the control of high harmonic generation via an APT. The quantum orbits contributing to each harmonic are characterized by their time of release into the continuum and their kinetic energy upon return to the ion core. The two most important orbits are those that have travel times τ_1 and τ_2 less than one optical cycle. Each orbit contributes to the dipole moment with a phase $\Phi_j = -\alpha_j(\tilde{\varepsilon})(U_p/\omega)$, where $\alpha_j(\tilde{\varepsilon})$ is the phase coefficient for the orbit τ_j, $\tilde{\varepsilon}$ is the return energy in units of the ponderomotive energy U_p, and ω is the IR laser frequency. For harmonics in the plateau, α_1 and α_2 differ by more than an order of magnitude, giving rise to very different time-frequency behaviors [6,7]. Macroscopic phase matching often favors one phase behavior over the other [3,8–10], but at the single atom level both components are always present and interfere. By using an APT to steer the electron to one trajectory or another, we can eliminate the interference and choose the spectral properties of the harmonics.

We calculate the time-dependent dipole moment for a helium atom interacting with an 810 nm fundamental field and an APT by solving the time-dependent Schrödinger equation in the single active electron approximation [11,12]. The total electric field is given by

$$E(t) = E_1(t)\sin\omega t + E_h(t - t_d)\sum_q \sin(q\omega[t - t_d] + \phi_q), \tag{1}$$

where the IR field envelope, $E_1(t)$, is a cosine function with a full width at half maximum (FWHM) in intensity of 27 fs, and the APT envelope, $E_h(t)$, is a $\cos^4$ function with a FWHM of 14 fs. We use an idealized train with odd harmonics 11–19 and relative phases $\phi_q = 0$, resulting in a train of 270 as pulses [13]. For most of the calculations we present, the IR peak intensity is 4×10^{14} W/cm^2 and the APT peak intensity is 10^{13} W/cm^2 [14]. The intensities have been chosen such that the ionization is enhanced by a factor of 20–25 for all values of the delay t_d, which means the APT dominates the ionization step. The ionization enhancement is linear in the APT intensity.

Our main result is summarized in Fig. 1. We plot the dipole spectrum calculated from $|\mathcal{A}(\omega)|^2/\omega^4$ where $\mathcal{A}(\omega)$ is the Fourier transform of the electron's acceleration [12]. For reference, the harmonic spectrum generated by the IR pulse alone is shown in blue in every panel. The plateau harmonics in this spectrum are not resolved. This is because the intensity dependence of the dipole phase gives rise to a characteristic time-dependent frequency (a chirp) for each quantum path. The chirp is negative, with a rate b_j proportional to $\alpha_j I_1/\mathcal{T}_1^2$ [15], where $\mathcal{T}_1$ and I_1 are the IR pulse duration and the peak intensity, respectively. These chirps induce a spectral broadening. Since α_j is large for the long quantum paths, the bandwidth of each harmonic is larger than 2ω for a 27 fs IR pulse.

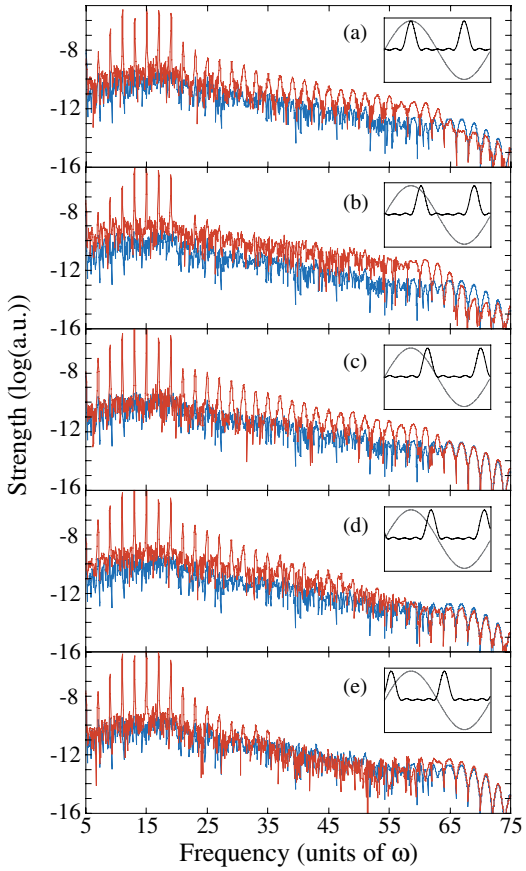

FIG. 1 (color). Harmonic spectra generated by a 4×10^{14} W/cm^2 IR pulse alone (blue lines), or in combination with a 10^{13} W/cm^2 attosecond pulse train (red lines), for five different values of the delay between the two pulses. The delays are, in units of the IR cycle, (a) $t_d = -0.25$, (b) $t_d = -0.16$, (c) $t_d = -0.094$, (d) $t_d = -0.063$, and (e) $t_d = +0.063$.

Figure 1 also shows harmonic spectra generated by the IR pulse in combination with an APT for various values of the delay time t_d, in units of the IR period T_1. The overlap between the IR field and the APT is shown in the insets. Both the strength and spectral resolution of the harmonics are altered by the presence and the timing of the APT. At some delays the plateau harmonics are enhanced by 1 to 2 orders of magnitude, while at others there is no enhancement at all. This variation in yield comes in spite of the fact that, as mentioned above, the ionization is enhanced at all delays. The yield and the resolution of the harmonics follow a progression as a function of t_d. At $t_d = -0.25$ [Fig. 1(a)], the harmonics in the plateau region are enhanced and spectrally resolved. The resolution then decreases as t_d increases, so that at $t_d = -0.16$ [Fig. 1(b)], the harmonics are enhanced but not spectrally resolved. After this, the resolution increases again, and at $t_d = -0.094$ [Fig. 1(c)] the spectrum is again well resolved. The enhancement and spectral resolution then gradually disappear, beginning with the high energy harmonics and moving to lower orders. At $t_d = -0.063$ [Fig. 1(d)], the spectrum is enhanced only through the 49th harmonic, and the enhancement is completely absent by the time t_d is $+0.063$ [Fig. 1(e)], except for the strong response at the train harmonics which is evident in all the spectra.

The most striking result in Fig. 1 is the spectral resolution of the plateau harmonics at the two "good" delays, $t_d = -0.25$ and $t_d = -0.094$. The presence of the APT seems to have eliminated the contributions from the longer quantum paths, selecting only the short quantum orbit to contribute to the harmonic generation process. This short path selection can be confirmed by analyzing the time-frequency behavior of the harmonics generated at these two delays. We evaluate the time-dependent frequency of each harmonic by windowing its spectrum and transforming to the time domain [12]. We find that each harmonic exhibits a single, linear frequency chirp. This would not be the case if there was more than one quantum path contribution to the dipole moment. In Fig. 2(a) we plot the chirp rate as a function of the harmonic order for a delay of $t_d = -0.094$, for three different IR intensities. The magnitude of the chirp rate increases with order for all three intensities. This is characteristic of the short quantum path, since α_1 increases as a function of the return energy. In contrast, α_2 decreases as a function of return energy. Furthermore, as we show below, the magnitudes of the harmonic chirps match very well those calculated for the short quantum path in the semiclassical

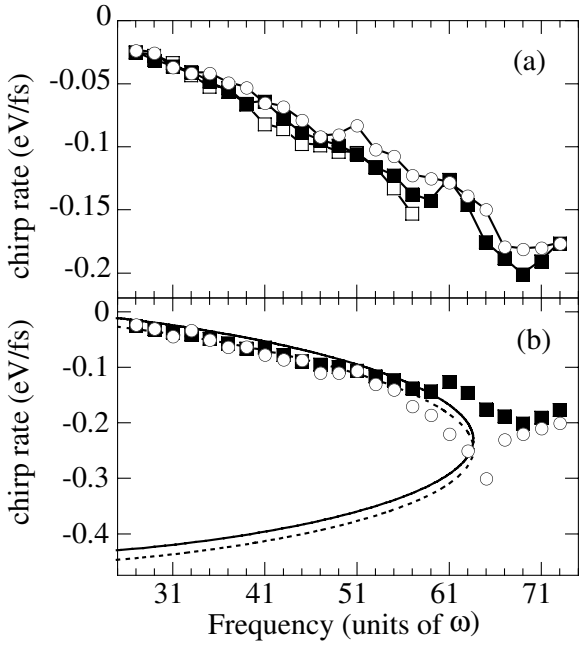

FIG. 2. (a) Chirp rates vs harmonic order for three different peak intensities of the IR pulse; $I_1 = 3 \times 10^{14}$ W/cm^2 (open squares), $I_1 = 4 \times 10^{14}$ W/cm^2 (solid squares), and $I_1 = 5 \times 10^{14}$ W/cm^2 (open circles). (b) Comparison of chirp rates of the full calculation (symbols) at the two good delays (see text) to those of the simple model (lines), for an IR intensity of $I_1 = 4 \times 10^{14}$ W/cm^2. We show both the downhill (solid squares/solid line) and the uphill (open circles/dashed line) results.

model. Finally, we note the slow intensity dependence of the chirp rate. As the intensity changes between 3×10^{14} W/cm^2, 4×10^{14} W/cm^2, and 5×10^{14} W/cm^2, the chirp rates for the plateau harmonics change by only ~20%. This is also typical of the short quantum path; b_j is proportional to the product $\alpha_j I_{\text{peak}}$, and since α_1 decreases with increasing intensity for a given harmonic [6,16], the chirp rate varies only slowly with intensity. Again, this is opposite to the behavior expected for the long quantum path. This slow intensity dependence means that the spectral narrowing and small chirp values that we observe in these single atom calculations will be relatively insensitive to the intensity variations in a real laser focus. We therefore predict that it will be experimentally observable.

To understand why varying the APT delay selects a particular quantum path, we examine the classical electron dynamics in the combined IR + APT electric field. We use the standard semiclassical model of harmonic generation [5], modified as follows. First, as we discussed above, we assume that the ionization step is entirely due to the APT. At higher IR intensities which approach saturation, this assumption will break down. Second, we modify the tunnel-ionization condition that the electron trajectories begin with zero initial velocity. Since ionization proceeds via one-photon absorption, the electron is released with a nonzero kinetic energy. We estimate this as $E_k(t_0) = E_0 + \bar{q}\omega - V(t_0)$ where E_0 is the ground state energy, $\bar{q}\omega$ is the average energy of the APT ($\bar{q} = 15$ here) and $V(t_0)$ is the height of the combined Coulomb + IR field barrier at the release time t_0 [17]. The subsequent electron dynamics are the same as in the standard model; the acceleration is imparted by the IR field, and only trajectories that return to the ion core give rise to harmonic generation.

The new feature of the APT + IR trajectory calculations is the inclusion of the electron's initial velocity $v(t_0)$ as an additional degree of freedom. There are now two families of classical trajectories the electron can follow, corresponding to $v(t_0)$ in the same direction as the IR field (uphill with respect to the combined potential because of the electron's negative charge), or in the opposite direction of the field (downhill with respect to the potential). The two families of trajectories are shown in Fig. 3 where we plot the return energy of the electron as a function t_0. Each family is characterized by a range of release times leading to either a short trajectory (solid line) or a longer trajectory (dotted line) that can include several returns. There are also release times that lead to no returning trajectories. Since the individual attosecond pulses have a duration of about $0.1T_1$, they can select a small range of release times and thereby determine which trajectories contribute to the spectrum.

This simple model can be used to qualitatively explain the trends in harmonic yield and spectral resolution that we discussed in connection with Fig. 1. When the electron is released at -0.25 [as in Fig. 1(a)], only the short uphill trajectories contribute to the harmonic spectrum. These α_1 contributions lead to a well resolved spectrum which is enhanced compared to the IR laser alone. As the release time increases, there is a region around $t_0 \sim -0.16$ [Fig. 1(b)] when only long trajectories contribute to harmonic generation, leading to enhancement of the spectrum with unresolved individual harmonics. For t_0 between approximately -0.125 and 0 [as in Figs. 1(c) and 1(d)], only short downhill trajectories will contribute to the spectrum, leading to well resolved harmonics. As the release time increases toward zero, the energy of the returning electrons decreases, meaning that only the low energy harmonics will be enhanced and resolved. Finally, when electrons are released after $t_0 = 0$, there are no returning trajectories initiated by the APT, and we therefore see no enhancement of the spectrum. The precise positions of the two families of trajectories are sensitive to the initial velocity. The simple model predicts the optimal delays for α_1 selection to be slightly too large for the uphill trajectories and slightly too small for the downhill trajectories. This means that our estimate of the initial velocity is somewhat too large. Reducing the initial energy by 10%–20% would give better agreement between Figs. 1 and 3.

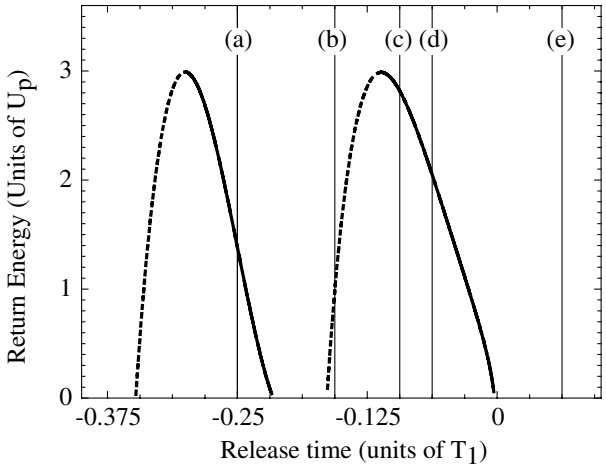

FIG. 3. Return energy as a function of the release time. Left hand curve: uphill trajectories; right hand curve: downhill trajectories. The IR intensity is 4×10^{14} W/cm^2. On each curve the long quantum path (α_2) is shown as a dotted line and the short quantum orbit (α_1) is shown as a solid line. The five labels (a)–(e) correspond to the panels in Fig. 1.

We can also use our analysis to quantitatively reproduce the harmonic chirp rates found in the full calculations. In Fig. 2(b) we calculate the chirp rates for the uphill and downhill short and long trajectories by integrating the classical action for the electron in the IR field [18]. The curves have an upper and a lower branch, corresponding to the α_1 (upper) and α_2 (lower) contributions. The comparison of the α_1 path chirp rates to those found in the full calculations at the good delays is excellent.

An experimental realization of APT quantum path control could begin by examining the spectrum of harmonics in a macroscopic phase matching configuration chosen to favor the short quantum path [19]. Adjusting the APT delay to an optimal value would then result in a large enhancement of the harmonic signal over the entire spectrum, since the single atom phase characteristics would be precisely matched to the macroscopic conditions. More generally, in any phase matching configuration, the spectral bandwidth of the harmonics will vary greatly as the electron trajectory is steered between the long and short quantum paths. We also expect that using more harmonics in the APT, leading to shorter attosecond bursts, would allow for selective enhancement of isolated parts of the harmonic spectrum.

Quantum path selection can also be applied to other strong field processes. For example, the high energy portion of the above threshold ionization (ATI) spectrum results from the elastic rescattering of electrons that return to the ion core [20]. As with harmonic generation, varying the delay of the APT would allow for the study of individual path contributions to the spectrum. In particular, when the IR laser is elliptically polarized, the ATI spectrum shows several plateaus which can be attributed to different quantum paths [5,21]. In addition, the extra degree of freedom introduced by the APT, the initial electron velocity, will cause new effects. Our calculations indicate that the photoelectrons resulting from uphill and downhill trajectories have different angular distributions. The uphill trajectory also yields a large number of orbits with low return energies (less than U_p). These make little contribution to the harmonic spectrum, and so we have omitted them from Fig. 3, but they should rescatter very efficiently.

Using an APT to launch electron trajectories with only a single return to the ion core could advance attosecond metrology beyond its present limits. When the τ_1 trajectory is selected, the return energy, as reflected in the emitted harmonic frequency, serves as a very high resolution attosecond "clock." In Fig. 1(c), the harmonics 31 through 63, corresponding to return energies between 1 and $3U_p$, receive their primary contributions from trajectories having return times spread over a 400 as interval, with the higher energies returning later. The 16 harmonic intervals thus define a 25 as clock division. By using a higher IR intensity the number of harmonics between 1 and $3U_p$ can be further increased, yielding even finer divisions.

In summary, we have shown that APTs are natural tools for controlling strong field processes. This is because their periodicity automatically matches that of the driving IR laser, allowing for the selection of different quantum path contributions. As a first application of this method, we have presented calculations that demonstrate the manipulation of the time-frequency characteristics of high harmonics at the single atom level.

K. S. acknowledges the support from the National Science Foundation through Grant No. PHY-9733890. A. H., J. B., and U. K. acknowledge support from the Bundesamt für Bildung und Wissenschaft, Switzerland through Grant No. 03.0010, and from the Swiss Quantum Photonics National Center of Competence in Research (QP-NCCR).

[1] P. M. Paul *et al.*, Science **292**, 1689 (2001).
[2] S. Harris, J. J. Macklin, and T. W. Hänsch, Opt. Commun. **100**, 487 (1993); G. Farkas and C. Toth, Phys. Lett. A **168**, 447 (1992).
[3] Ph. Antoine, A. L'Huillier, and M. Lewenstein, Phys. Rev. Lett. **77**, 1234 (1996).
[4] M. Lewenstein, Ph. Balcou, M. Yu. Ivanov, A. L'Huillier, and P. B. Corkum, Phys. Rev. A **49**, 2117 (1994).
[5] P. Salières *et al.*, Science **292**, 902 (2001).
[6] M. Bellini, C. Lyngå, A. Tozzi, M. B. Gaarde, T. W. Hänsch, A. L'Huillier, and C.-G. Wahlström, Phys. Rev. Lett. **81**, 297 (1998).
[7] M. B. Gaarde *et al.*, Phys. Rev. A **59**, 1367 (1999).
[8] P. Salières, A. L'Huillier, and M. Lewenstein, Phys. Rev. Lett. **74**, 3776 (1995).
[9] L. Nugent-Glandorf *et al.*, Phys. Rev. A **62**, 023812 (2000).
[10] M. B. Gaarde and K. J. Schafer, Phys. Rev. A **65**, 031406(R) (2002).
[11] K. C. Kulander, K. J. Schafer, and J. L. Krause, in *Atoms in Intense Laser Fields*, edited by M. Gavrila (Academic Press, San Diego, 1992).
[12] K. J. Schafer and K. C. Kulander, Phys. Rev. Lett. **78**, 638 (1997).
[13] Calculations with experimentally determined phases [1] give the same results at slightly different delays t_d.
[14] E. Constant *et al.*, Phys. Rev. Lett. **82**, 1668 (1999). The intensities of the harmonics were estimated assuming a 27 fs pulse with 2 mJ energy in the IR and an efficiency of 4×10^{-5} for the 15th harmonic in xenon.
[15] M. B. Gaarde, Opt. Express **8**, 529 (2001).
[16] Ph. Balcou, A. S. Dederichs, M. B. Gaarde, and A. L'Huillier, J. Phys. B **32**, 2973 (1999).
[17] J. Wassaf, V. Véniard, R. Taïeb, and A. Maquet, Phys. Rev. Lett. **90**, 013003 (2003).
[18] C. Kan, C. E. Capjack, R. Rankin, and N. H. Burnett, Phys. Rev. A **52**, R4336 (1995).
[19] S. Kazamias *et al.*, Phys. Rev. A **68**, 033819 (2003).
[20] K. J. Schafer, B. Yang, L. F. DiMauro and K. C. Kulander, Phys. Rev. Lett. **70**, 1599 (1993).
[21] G. G. Paulus, F. Zacher, H. Walther, A. Lohr, W. Becker, and M. Kleber, Phys. Rev. Lett. **80**, 484 (1998).